Jour. of the KGS Vol. 16, No 3, June 2000, pp 77-88

Numerical Analysis of Stress-Strain Behavior of Geofoam

지오폼의 응력-변형률 거동의 수치적 해석

Chun, Byung-Sik[*1] 천 병 식 Lim, Hae-Sik[*2] 임 해 식
Ahn, Tae-Bong[*3] 안 태 봉 Lee, Cheol-Kyu[*4] 이 철 규

요 지

연약지반상에 하중 경감을 목적으로 발포성 폴리스티렌(Expanded Polystyrene)을 사용하는 사례가 최근 꾸준히 증가하고 있다. 공법의 요점은 연약지반상에 축조되는 상부구조물에 의한 응력증가를 감소시켜서 결국에는 침하를 방지하기 위한 것이다. 이것을 지오폼(geofoam)이라고 하는데, 지오폼은 교대나 옹벽의 뒷채움재로 사용할 경우 횡토압을 감소시키기 때문에 옹벽이나 교대의 뒷채움재료로 사용하기도 한다. 이와 같이 그 사용이 꾸준히 증가하고 있지만 뒷채움이나 연약지반상에 사용할 때 지오폼의 거동을 예측하는 적절한 수치모델이 아직은 개발되지 않았다. 본 연구에서는 지오폼의 응력-변형 특성을 연구하고 그 탄소성 예측모델을 제시하였다. 이를 위하여 삼축압축시험을 실시하였으며 구속응력과 지오폼의 밀도를 다양하게 변화시켜 그 응력-변형특성을 조사하고 회귀분석을 통하여 비선형 구성모델을 제시하였다. 그 결과 지오폼은 탄성 선형모델보다 탄소성모델 특성에 더 가까운 것을 알 수 있었으며 체적변화율과 축방향 변형률에는 특별한 상관 관계가 있음을 알 수 있었다.

Abstract

The use of geofoam block is consistently increasing as a filling material on soft ground. The beneficial effect of geofoam is due to minimizing the stress increment, which, in turn, reduces the settlement. The geofoam can also be used as a backfill material for retaining walls and abutments to reduce the lateral earth pressure. However, the prediction of the geofoam behavior that is essential for the selection of the filling configuration and the settlement estimation has not been studied, and prediction model has not been developed yet. In this paper, the nonlinear numerical constitutive model of geofoam is suggested from the results of triaxial compression tests. Triaxial tests were performed by varying the density and confining stresses, and regression analysis were performed. From this study, it was found that elasto-plastic behavior is more appropriate to predict settlement or deformation of geofoam, and there is special relationship between volume strain and axial strain.

Keywords : Constitutive model, Geofoam, Regression, Elasto-plastic

1. Introduction

There are many soil improvement methods concerning bearing capacity and shear strength of soils. When soil fills or structures need to be constructed on the site like soft ground or slopes of which bearing capacity and shear strength arenot sufficient to endure applied load, the geofoam method has several advantages such as light weight, self standing characteristics, easy handling, and short period of construction. Most of the advantages of

*1 Professor. Dept. of Civil Engrg., of Hanyang Univ.
*2 Senior Researcher, Office of Korea National Housing Co.
*3 Assistant Professor, Dept. of Civil and Environmental Engrg., Woosong Univ
*4 Graduate Student, Dept. of Civil Engrg., Chungang Univ.

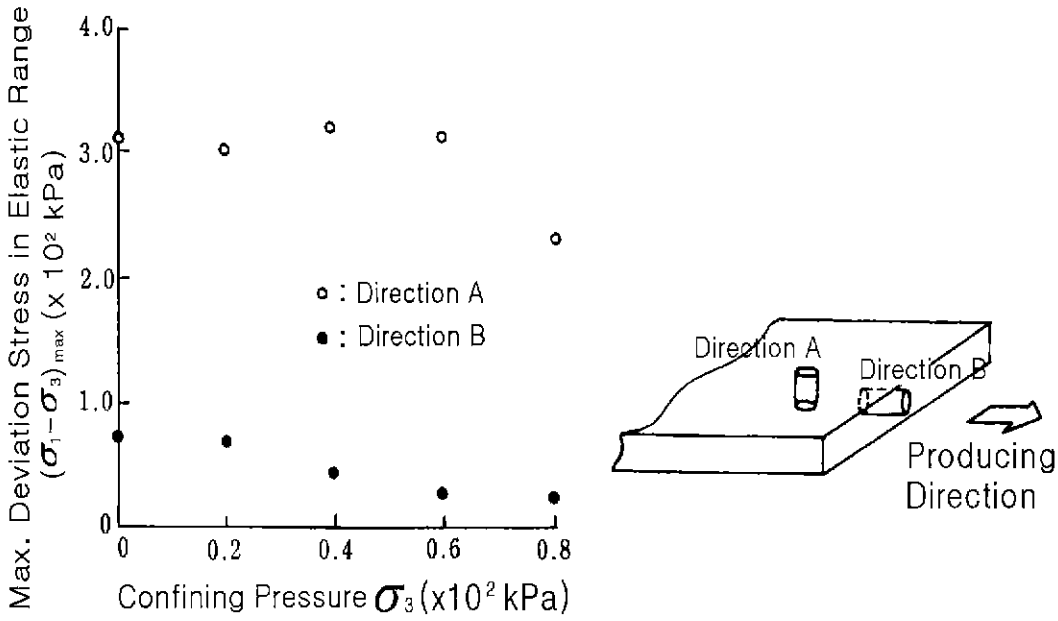

Fig. 1 Difference of strength by production direction of geofoam (From EPS construction method development organization, 1993)

geofoam method are fundamentally caused by lightweight of geofoam that weighs only 0.2~0.35 kN/m^3.

Geofoam block behaves different manner with soils; (1) the stress-strain behavior of geofoam is distinguished due to its low density (2) geofoam behavior is time dependent and mechanically anisotropic.

Geofoam block should have appropriate strength to endure overburden stress, and exact stress-strain behaviors of geofoam filling have to be predicted in order to decide effective installation shape and area.

In this paper, stress-strain model of geofoam is developed as a function of overburden stress so that we could suggest properly geofoam density and replacement area for field application.

2. Review of Geofoam Characteristics

Anisotropy property of geofoam is one of the most important properties, but it is easily disdained. The stress-strain behavior of geofoam varies with producing direction (Kutara et al., 1989, Fig. 1). The direction of stress on the geofoam perpendicular to producing is more effective.

The geofoam typically shows elasto-platic behavior as shown in Fig.1 showing linear behavior in the strain range from 1% to 1.5% (Fig. 2). As geofoam density increases, the modulus and axial stresses increase not showing clear apex.

According to Hamada and Yamanouchi (1989), the volume of geofoam decreases linearly during compression (Fig. 3). Namely, the volume change rate is constant, and depends on the density of geofoam and lateral pressure applied.

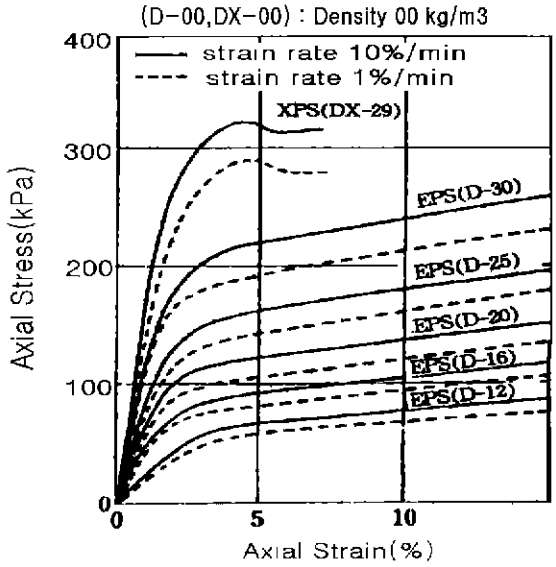

Fig. 2 Typical stress-strain curve of geofoam(From EPS construction method development organization, 1993)

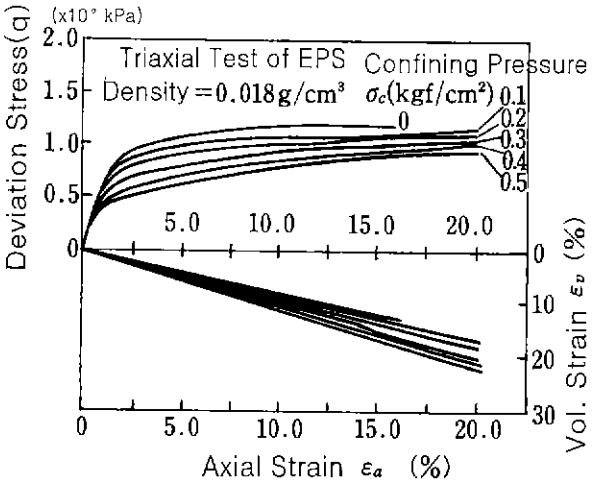

Fig. 3 Volume change characteristics of geofoam (From Hamada and Yamanouchi, 1989)

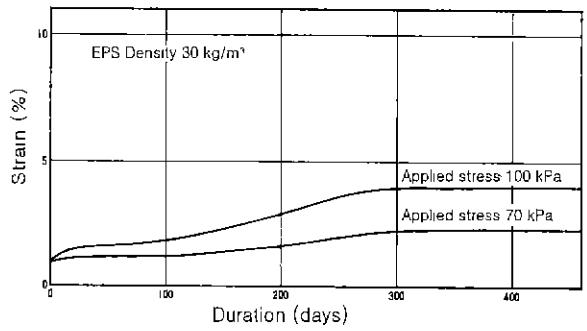

Fig. 4 Creep characteristics of geofoam(From EPS construction method development organization, 1993)

Another important property of geofoam is time dependent stress-strain behavior. According to previous researches (CMDO, 1993; Chun et al., 1996; Horvoth, 1998), strain of geofoam increase with applied stress that maintains for long duration as the same stress level (Fig. 4, Fig. 5, Fig. 6). The amount and duration of creep depend on geofoam density and level of applying stress (Horvoth, 1998). Therefore, these facts indicates that geofoam have to be used under adequate stress level in practical situation.

3. Numerical Model of Geofoam and Proposed Model

3.1 Geofoam Model

The geofoam behavior model has two kinds, one is for

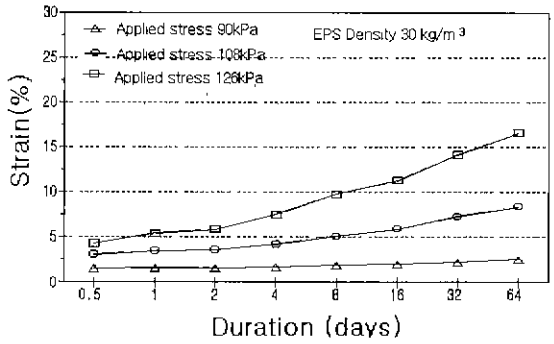

Fig. 5 Creep characteristics of geofoam (From Chun et al., 1996)

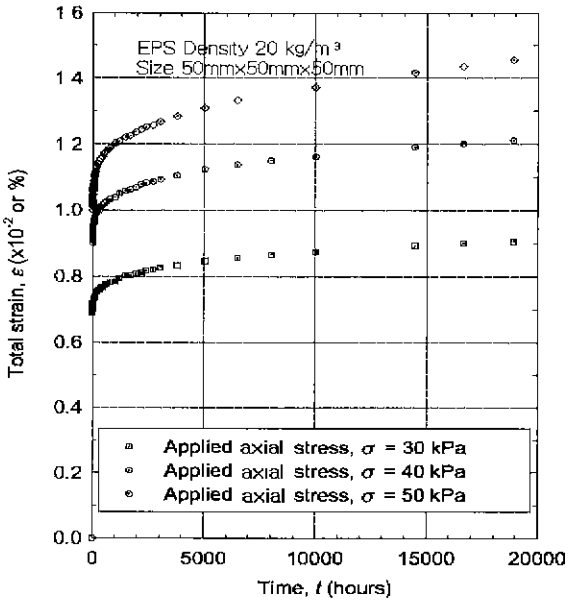

Fig. 6 Creep characteristics of geofoam (From Horvoth, 1998)

instantaneous behavior and the other one is long time behavior. The former also has two kinds; linear elastic model using initial tangential modulus and nonlinear model. Instantaneous nonlinear model was developed by Cho (1992) as shown in Fig. 7, and the corresponding equations are expressed in Eq. (1) and Eq. (2). In this model, elasto-plastic stress-strain behavior of geofoam, which is related with density and confining stress is depicted with parameters C, I, E_i, E_p, and Y_0 (Fig. 7). The Poisson's ratio that is important property in numerical analysis to calculate total volume change, is suggested as a function of confining stress as shown in Eq. (2).

$$\sigma_1 = (1 + E_p\varepsilon)\left[1 - \exp\left(-c\,\varepsilon^2 - \frac{E_i}{I}\right)\right] \quad (1a)$$

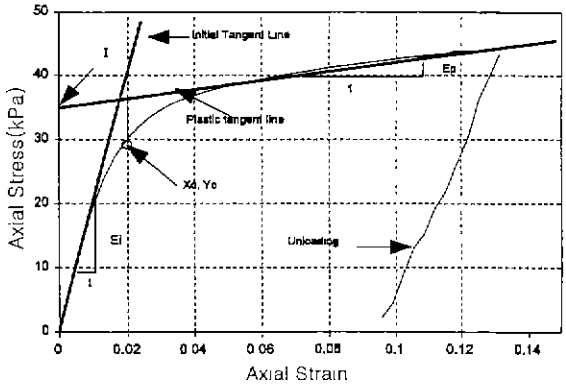

Fig. 7 Parameters to depict stress-strain relation (From Cho, 1992)

$$c = -\frac{E_i}{l\,Xo} - \frac{-1}{X_0^2}\ln\left[1-\frac{Y_0}{(I+E_p X_0)}\right] \quad (1b)$$

$$I = (-107+910\gamma)+(0.63-0.32\gamma)\,\sigma_3 \quad (1c)$$

$$E_i = (-4180+39000)+(-6.2-53\gamma)\,\sigma_3 \quad (1d)$$

$$E_p = (104+440\gamma)+(-3.6+150\gamma)\,\sigma_3 \quad (1e)$$

$$Y_0 = (1.4+905\gamma)+(-1.1+4.5\gamma)\,\sigma_3 \quad (1f)$$

$$\mu = 0.2-0.5\frac{\sigma_3}{62\text{kpa}} \quad \text{for} \quad 0 \le \sigma_3 \le 62\text{kPa} \quad (2)$$

where, σ_1 : Axial stress (kPa)

ε : Axial strain

γ : Unit weight of geofoam (kN/m^3)

σ_3 : Confining stress (kPa)

μ : Poisson's ratio

3.2 Proposed Nonlinear Numerical Geofoam Model

Geofoam is useful material that could replace the ground so that it can take advantages of lightweight property. Prediction of geofoam behavior using proper numerical model is essential in soils. As described in previous section, geofoam behavior is related deeply with density and applied stresses, both maximum and minimum principal stresses of geofoam. However, rational geofoam behavior prediction model including concerned all factors has not been developed yet. In this paper, nonlinear elastic geofoam model is suggested in instantaneous loading state. Triaxial compression tests with various densities and confining pressure of geofoam were executed to achieve the purpose.

4. Experiment

The samples for experiments prepared with four different densities of 0.147kPa, 0.196kPa, 0.245kPa, 0.294kPa. The samples were trimmed as cylindrical shape, diameter of 50 mm and height of 100mm, and a series of compression test were performed.

4.1 Procedures

The geofoam sample was prepared by cutting the geofoam material perpendicular angle as shown in A direction in Fig. 1. The samples were made by using cutting sampler. The cutting sampler has very sharp shape at two edges to trim samples so that soil sampler has a cylindrical shape, and the sample was cut by driving the sampler. By using this procedure, geofoam samples of smooth surface could be obtained. The axial load is applied to different specimens of various densities. Also, confining stresses were varied as 0, 20, 40, 60kPa. The speed of axial load was maintained at the value of 1 mm/min. The specimens were in drained condition during the test, and the volume change of geofoam during test was measured by checking discharged water volume from triaxial cell and the rubber membrane enveloping specimen to calculate Poisson's ratio. The experimental device was controlled by personal computer.

4.2 Results

The axial stress-strain relations obtained through triaxial apparatus are shown in Fig. 8 with the variation of geofoam densities and confining stresses. The analysis

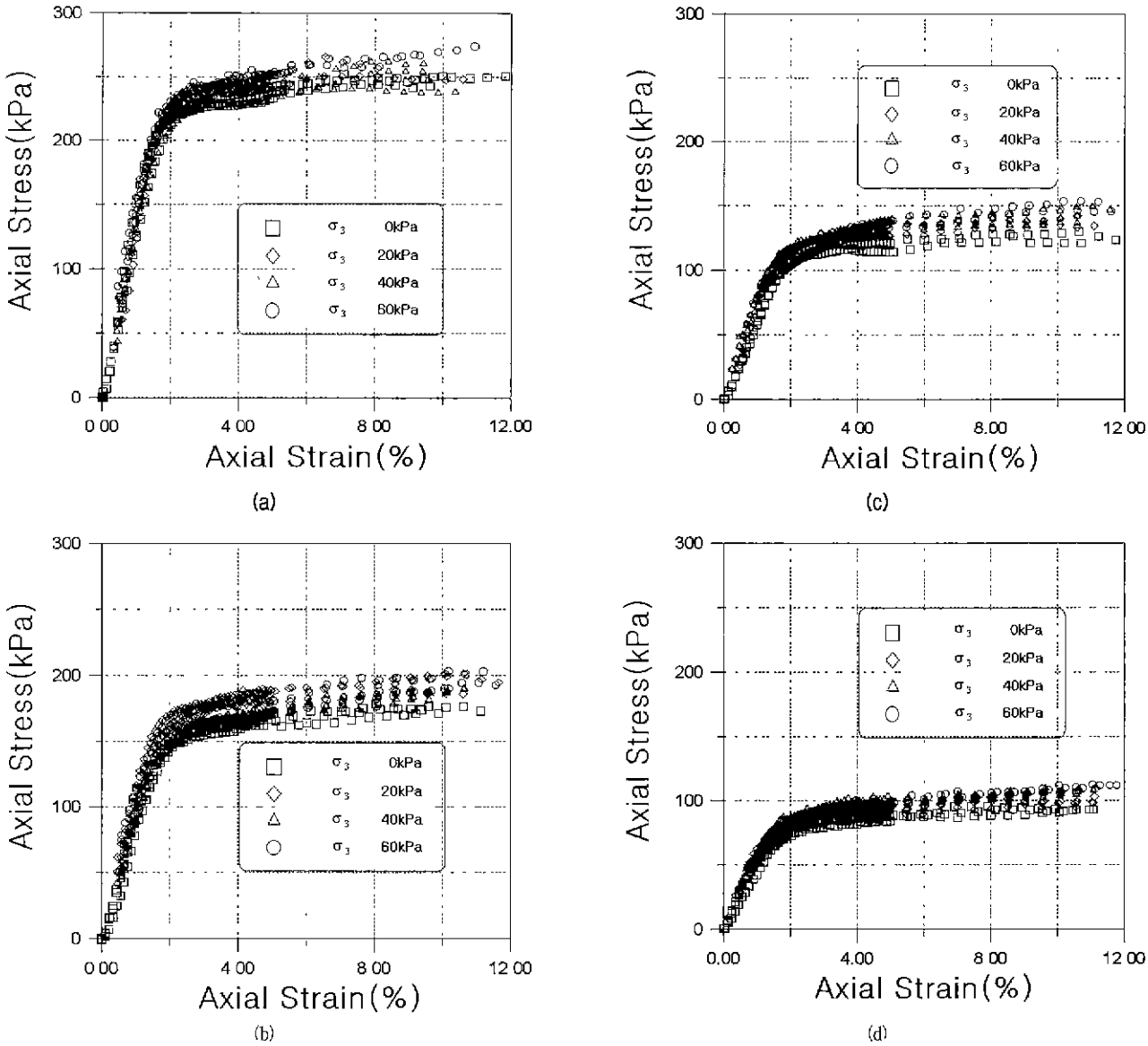

Fig. 8 Triaxial test results of axial stress-strain relation (a) density = 0.294 kN/m3 (b) density = 0.245 kN/m3 (c) density = 0.196 kN/m3 (d) density = 0.147 kN/m3

and prediction by proposed model are shown in Fig. 9, Fig. 10, Fig. 11, and Fig. 12. Also, the experimental axial strain and volumetric strain relations are shown in Fig. 12.

4.3 Stress-Strain Relations

The stress-strain relation of geofoam is closely linked to its density and confining stress. As density and confining stress increase, the axial stress and initial tangential modulus increase as shown in Fig 8. The stress-strain relation to represent stress-strain behavior of geofoam is proposed in Eq. (3) based on experimental results.

$$\sigma_1 = \frac{a\varepsilon_1^{\,b}}{c + \varepsilon_1^{\,b}} \tag{3}$$

where, σ_1 : axial stress

ε_1 : Axial strain

a, b, c : material parameter

The material parameter a, b and c varied with density and confining stress of geofoam, and the stress-strain curves depended on each parameter shown nonlinear form as shown in Fig. 8. The characteristics of Eq. (3) are shown in Fig. 10. This stress-strain relation depicts well elasto-plastic behavior of geofoam.

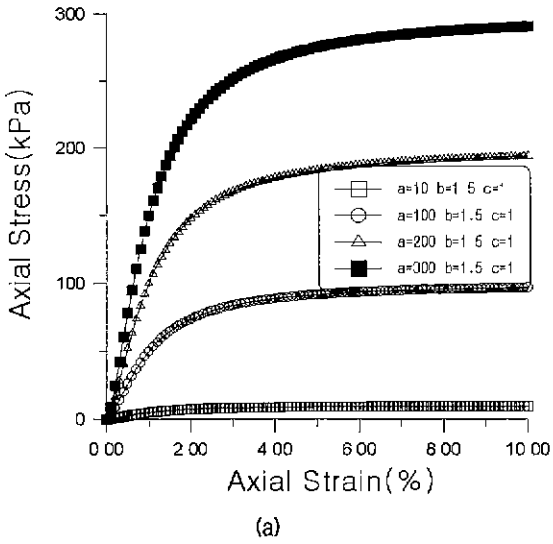

(a)

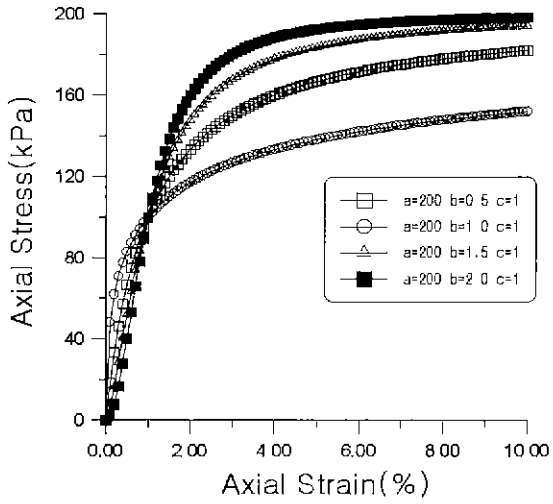

(b)

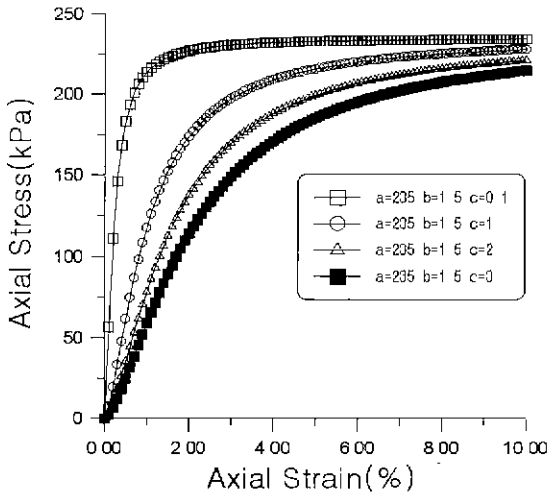

(c)

Fig. 9 The properties of parameters of proposed stress-strain relation (a) Parameter a (b) Parameter b (c) Parameter c

The comparisons of stress-strain behaviors of various densities of geofoam (i.e. 0.196kN/m^3, 0.294kN/m^3) and relations between laboratory measurement and regression results with proposed model are shown in Fig. 10. The results of comparisons between measurement and regression curve show good agreement.

The material parameters of a, b and c obtained by regression analysis of test results are described in Eq. 3 The parameter a, b and c can be expressed as a function of confining stress and geofoam density. This means that the stress and strain are function of confining stress and geofoam density, which means that the stress and strain are function of confining stress and geofoam density.

The relations between parameters and geofoam density and confining stress are shown in Eq. 4.

$$a = -60.955 + 9.843 \times d + 0.339 \times \sigma_3 \qquad R = 0.982 \tag{4a}$$

$$b = 1.135 + 0.0042 \times d - 0.008 \times \sigma_3 \qquad R = 0.800 \tag{4b}$$

$$c = -0.437 + 0.102 \times d - 0.002\, d^2 + 0.011 \times \sigma_3 - 0.389 \times d \times \sigma_3 \qquad R^2 = 0.31 \tag{4c}$$

where, d : density of geofoam (kg/m^3)
σ^3 : Confining stress (kPa)
R : correlation coefficient
R^2 : coefficient of determination

The statistic analyses of various tests show that minimum correlation coefficient is 0.99. Therefore, Eq. (3) describes axial stress-strain behavior of geofoam successfully (Table 1). The parameter a and b have multi-linear relation with geofoam density and confining stress, and the correlation coefficient, R, of a and b are 0.982 and 0.800 respectively. On the other hand, the coefficient of determination of parameter c is only 0.31.

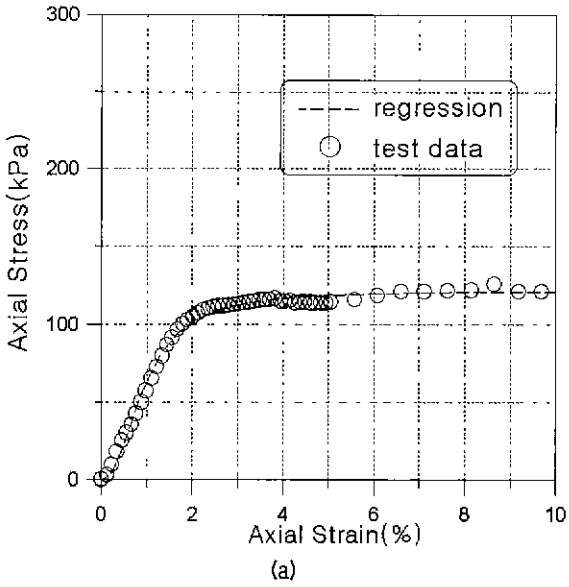
Axial Stress(kPa)
Axial Strain(%)
regression
test data
0
100
200
300
0
2
4
6
8
10
(a)

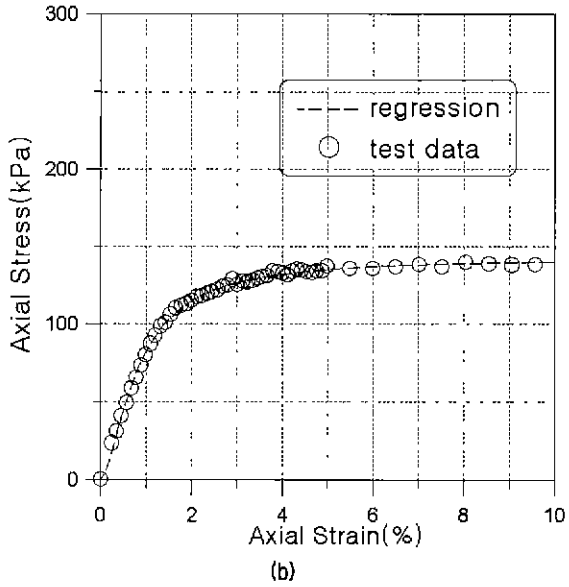
Axial Stress(kPa)
Axial Strain(%)
regression
test data
0
100
200
300
0
2
4
6
8
10
(b)

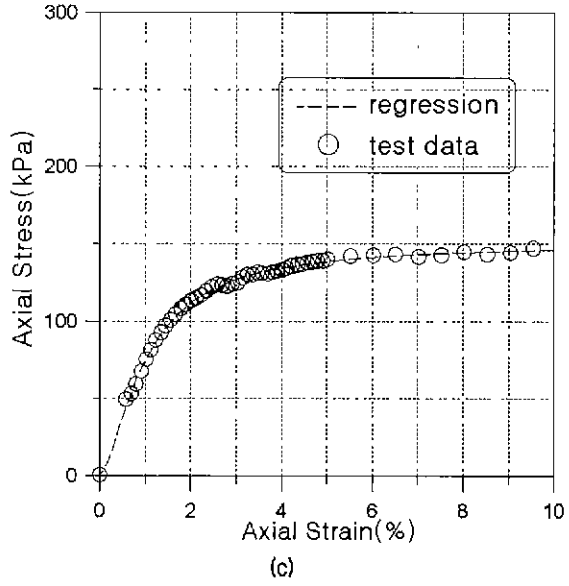
Axial Stress(kPa)
Axial Strain(%)
regression
test data
0
100
200
300
0
2
4
6
8
10
(c)

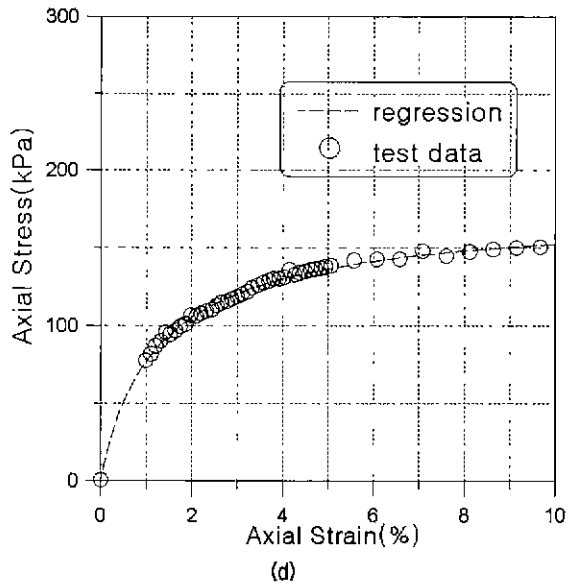
Axial Stress(kPa)
Axial Strain(%)
regression
test data
0
100
200
300
0
2
4
6
8
10
(d)

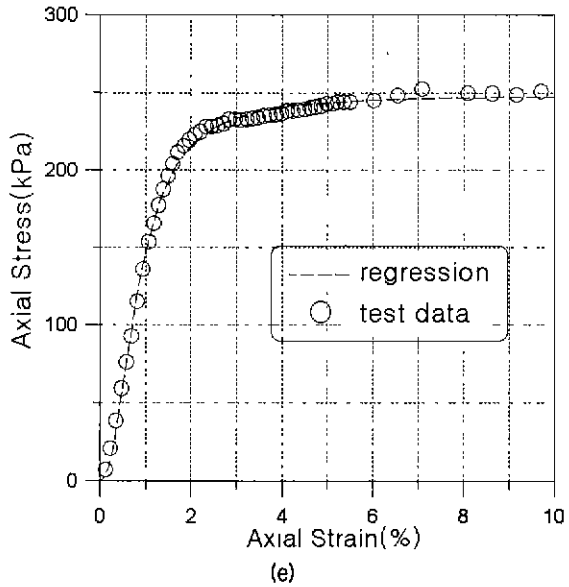
Axial Stress(kPa)
Axial Strain(%)
regression
test data
0
100
200
300
0
2
4
6
8
10
(e)

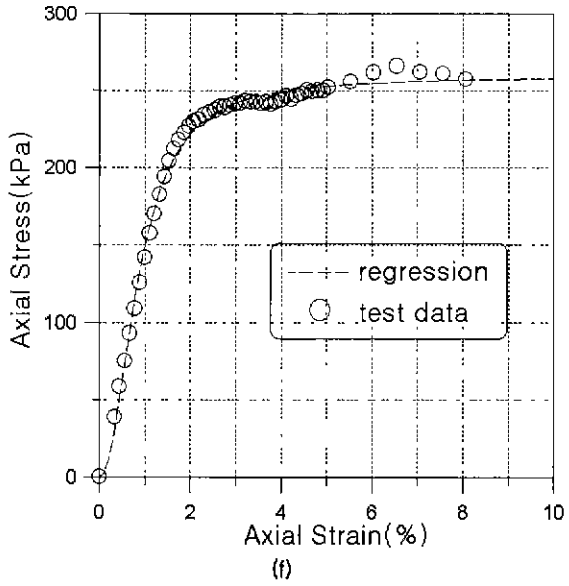
Axial Stress(kPa)
Axial Strain(%)
regression
test data
0
100
200
300
0
2
4
6
8
10
(f)

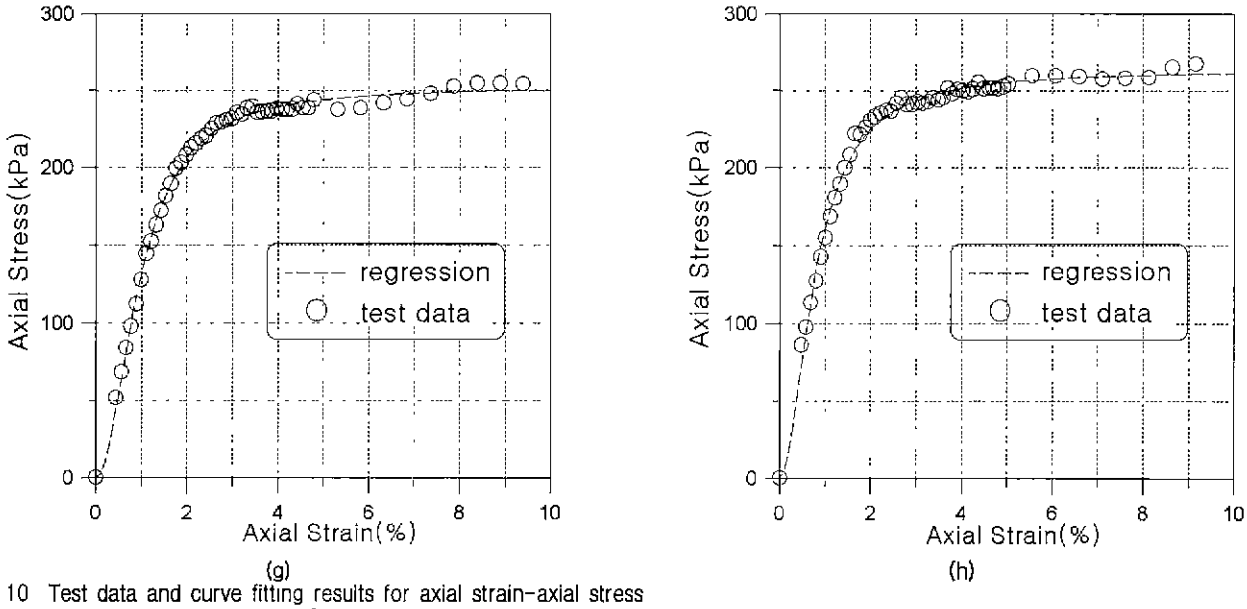

Fig 10 Test data and curve fitting results for axial strain-axial stress

(a) density 0.196kN/m3, σ^3 = 0 kPa R = 0.9969 (b) density 0.196kN/m3, σ^3 = 20 kPa, R = 0.9989
(c) density 0.196kN/m3, σ^3 = 40 kPa, R = 0.9989 (d) density 0.196kN/m3, s3 = 60 kPa, R = 0.9982
(e) density 0.294kN/m3, s3 = 0 kPa, R = 0.9978 (f) density 0.294kN/m3, s3 = 20 kPa, R = 0.9977
(g) density 0.294kN/m3, s3 = 40 kPa, R = 0.9986 (h) density 0.294kN/m3, s3 = 60 kPa, R = 0.9977

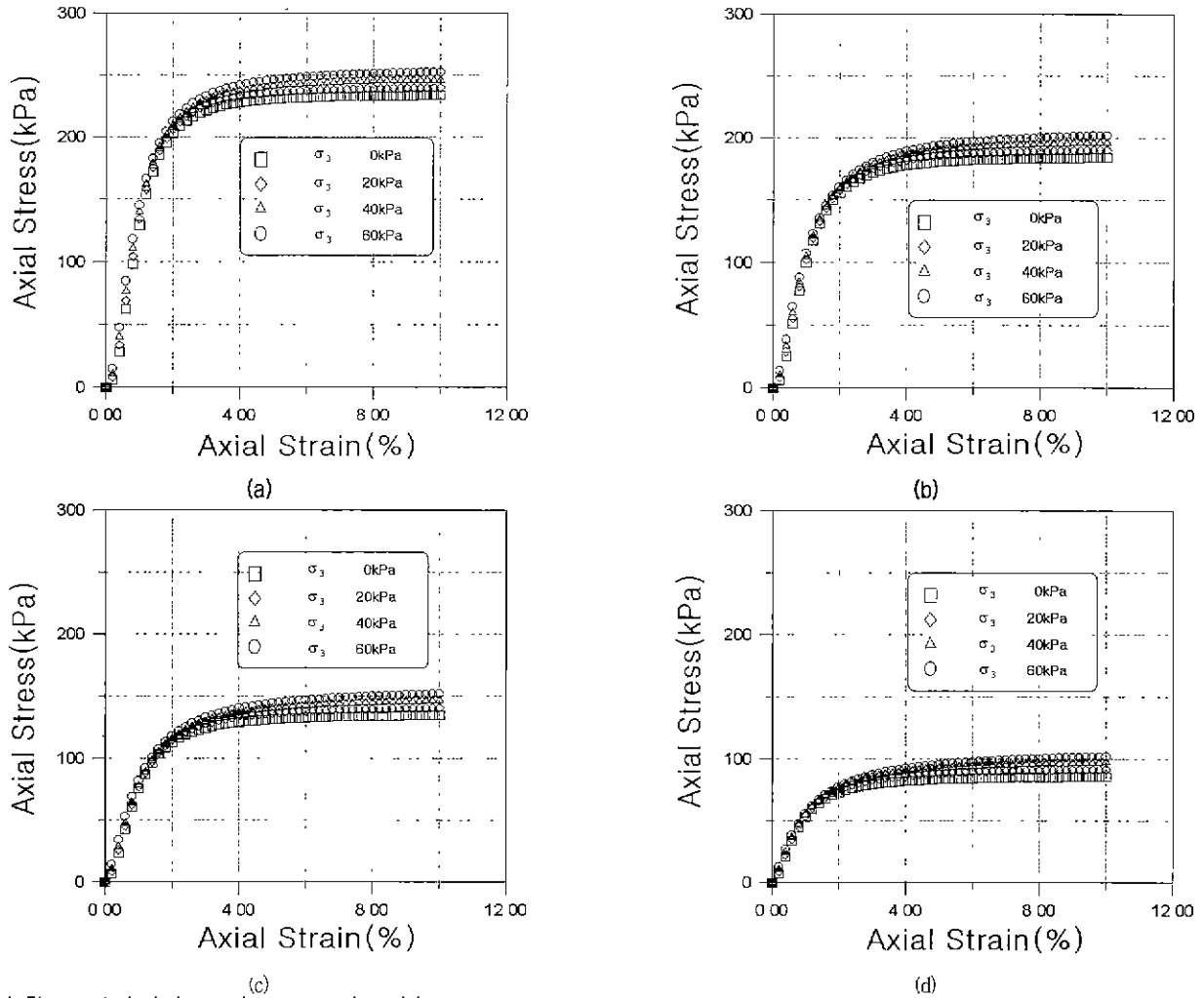

Fig.11 Stress-strain behavior by proposed model

(a) Density = 0.294 kN/m^3 (b) Density = 0.245 kN/m^3 (c) Density = 0.196 kN/m^3 (d) Density = 0.147 kN/m^3

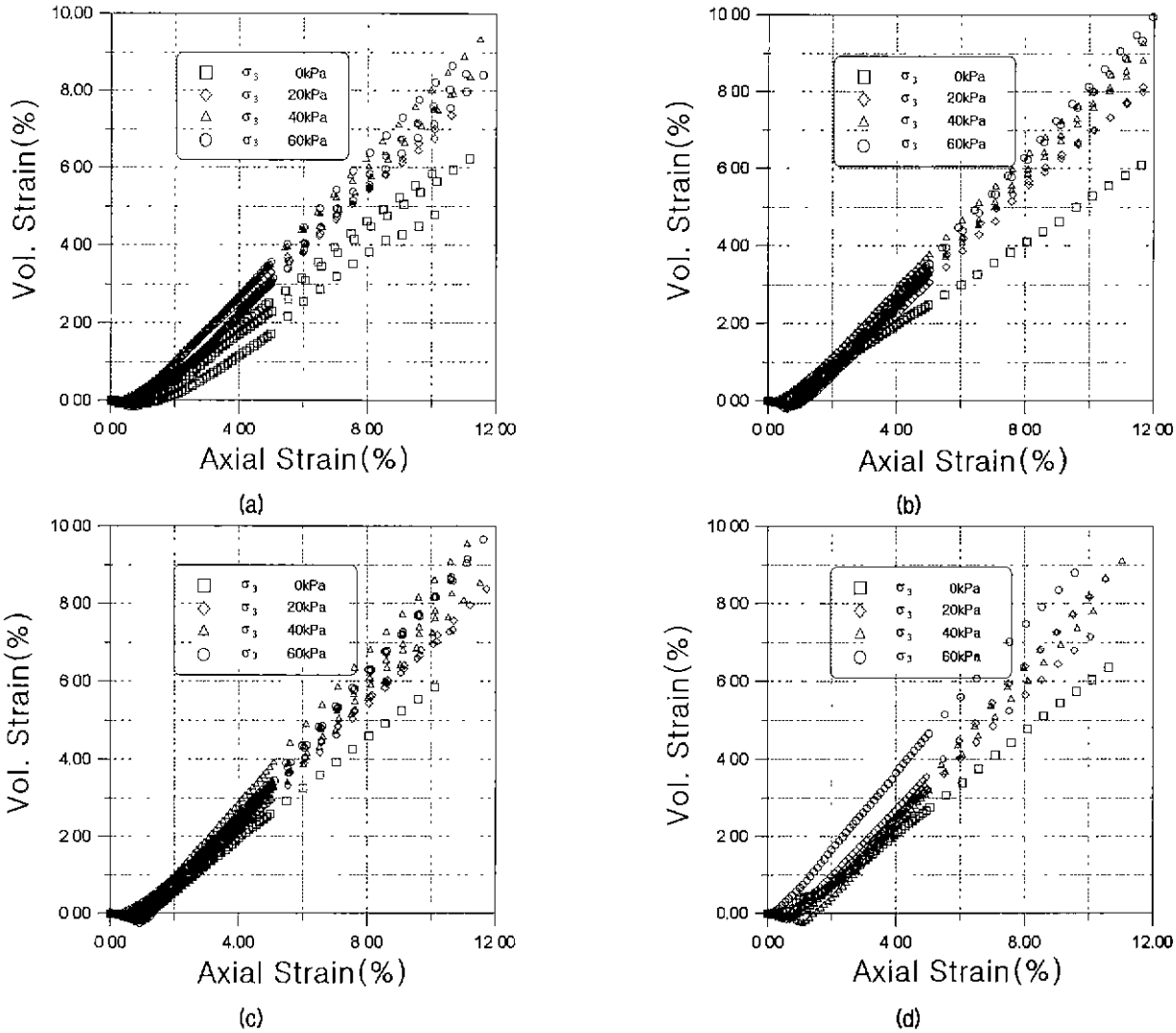

Fig. 12 Triaxial test results of axial strain versus volumetric strain relation
(a) density = 0.294 kN/m^3 (b) density = 0.245 kN/m^3 (c) density = 0.196 kN/m^3 (d) density = 0.147 kN/m^3

The reason is that the range of parameter c is low with the value of 0.814 ~ 0.929 while a varies from 105.84 to 265.07, and b is 0.966 ~ 2.86 (Table 1). However, since the contribution of parameter c to form the stress-strain curve of geofoam is relatively small (Fig. 9), the reliability of Eq. (3) is satisfied. Also, it could be verified comparing Fig. 8 with Fig 11 described by Eq. (3) and Eq. (4). The stress-strain behavior of geofoam well coincide with predicted behavior by proposed model.

The derivative of Eq. (3), which is tangential modulus at each stress level, can be expressed as Eq. (5).

$$E_t = \frac{abc\varepsilon_1^{b-1}}{\varepsilon_1^{2b} + 2c\varepsilon_1^{b} + c^2} \qquad (5)$$

where, E_t : tangential modulus

ε_1 : Axial strain

a, b, c : Parameters concerned with density and confining stress

The volume change of geofoam

The volumetric strain of geofoam has a linear relation with axial compression strain as shown in Fig. 12, and the slope of Fig. 12 has a correlation with density and confining stress of geofoam.

The regression analysis of the relation between volumetric strain and axial compression strain concerning with the density and confining stress of geofoam in Fig. 12 shows that correlation coefficient is at least 0.9934 (Table 2).

Table 1. The statistic analysis of triaxial test data of EPS on stress-strain relation

Density (t/m^3)	Confining Stress kPa	curve fitting of test results on proposed function : equation (3)				prediction of parameter a,b,c by equation (4)		
		a	b	c	상관 계수	a	b	c
0.294	0	238.584	2.2	0.537*	0 9985	234 347	2 394	0.814
0.294	0	248.515	2.17	0 684	0 9988	234 347	2.394	0.814
0.294	0	248.044	2.06	0 901	0 9978	234.347	2 394	0.814
0.294	20	246.71	2.86	0 985	0 9978	241.127	2 234	0.794
0.294	20	261.202	2 18	1 190*	0.9968	241.127	2 234	0.794
0.294	20	258.959	2 12	0.726	0.9977	241.127	2 234	0.794
0.294	40	252 528	2 01	0.900	0.9986	247.907	2.074	0.773
0.294	40	255.185	2.48	0 864	0.9973	247.907	2.074	0.773
0.294	40	236 599	2 45	0.567	0.9978	247.907	2 074	0.773
0.294	60	263 031	1 88	0 629	0.9977	254.687	1 914	0.753
0.294	60	265 07	1.95	0.829	0.9958	254.687	1 914	0.753
0.245	0	174.611	2 01	0 875	0.9985	185.13	2.184	0.857
0.245	0	167 971	2 01	0.69	0.9985	185.13	2 184	0.857
0.245	0	173.444	2.30	1 114*	0.9989	185.13	2 184	0 857
0.245	20	196 215	1 84	0 637*	0.9972	191.91	2.024	0.875
0.245	20	197.153	1 94	0 972	0.9984	191.91	2.024	0.875
0.245	20	187.599	1 92	0.726	0 9984	191.91	2.024	0.875
0.245	40	179.574	2 13	1 031	0.9961	198.69	1.864	0.893
0.245	40	179.972	1 807	0.95	0.9949	198.69	1 864	0.893
0.245	40	185.094	1 75	0 811	0 9958	198.69	1.864	0.893
0.245	60	196.225	1 42	1.062	0.9937	205.47	1.704	0.912
0.245	60	183.996	1 542	0 599*	0 9912	205.47	1.704	0.912
0.245	60	195.417	1 739	0.715	0 9910	205.47	1 704	0.912
0.196	0	127.718	2 2	0 967	0 9974	135.913	1.974	0.799
0.196	0	121.901	2 203	0.928	0 9969	135.913	1 974	0.799
0.196	20	142.91	1.591	0 737	0 9989	142.693	1 814	0.856
0.196	20	132.287	2 281	0 823	0.9983	142.693	1.814	0.856
0.196	40	134.355	1 805	0 584*	0.9947	149.473	1.654	0.913
0.196	40	150.003	1 565	1 007	0 9989	149.473	1.654	0.913
0.196	40	142.382	1.873	0.716	0.9949	149.473	1.654	0.913
0.196	60	161.188	0.966	1.062	0.9986	156.253	1.494	0.970
0.196	60	174.163	0.945	1.257*	0.9982	156.253	1 494	0.970
0.147	0	91 812	1.435	0 739	0 9983	86 696	1 765	0.640
0.147	0	92.381	1.805	0 624	0 9994	86 696	1 765	0.640
0.147	20	97 642	1.487	0.786	0.9963	93 476	1.605	0.736
0.147	20	100.209	1.749	0.693	0.9967	93 476	1.605	0.736
0.147	20	99 255	1.674	0 584	0 9958	93 476	1 605	0.736
0.147	40	104.817	1.568	0.696	0.9940	100.256	1.445	0.833
0.147	40	108.622	1.528	0 773	0 9962	100 256	1 445	0.833
0.147	40	105.837	1.37	0 896	0 9902	100 256	1.445	0.833
0.147	60	108.696	1.346	0.938	0.9957	107.036	1.285	0.929
0.147	60	112.109	1.489	1.190*	0 9955	107.036	1 285	0.929
0.147	60	115.817	1.25	1 042	0 9855	107 036	1 285	0.929
0.147	60	108.786	1.300	0.958	0.9944	107 036	1.285	0 929

* excluded data in regression analysis of c

Also, the Poisson's ratio can be expressed as shown in Eq. (6).

$$v = \left(1 - \frac{\varepsilon_v}{\varepsilon_1}\right) \tag{6}$$

Where, v : Poisson's ratio

ε_v : Volumetric strain

ε_1 : Axial strain

It is easily inferred that Poisson's ratio has a multi-linear relation with density and confining stress of geofoam based on Eq. (6) and test results. The results of static analysis of relations can be expressed as shown in Eq. (7), and details are described in table 2.

$$v = 0.0967 + 0.0031 \times d - 0.0023 \times \varepsilon_3 \tag{7}$$

Where, v : Poisson's ratio

Table 2. Statistic analysis results of poisson's ratio

Density (t/m^3)	Confining Stress	Vol. Strain /axial strain	R	calculation of poisson ratio by Eq. (6)	prediction of poisson ratio by Eq (7)
0 03	0	0.59	0.9934	0 2050	0 189332
0.03	0	0.6533	0.9995	0 1733	0.189332
0.03	0	0.6478	0.9983	0.1761	0.189332
0.03	20	0 7339	0 9985	0.1326	0.142977
0.03	20	0.7735	0 9985	0.1133	0.142977
0.03	30	0.8446	0.9997	0 0777	0 119800
0.03	40	0.8235	0.9991	0.0883	0.096623
0.03	40	0.8323	0.9986	0.0838	0.096623
0.03	40	0.8686	0.9995	0.0674	0.096623
0.03	60	0.8713	0 9996	0.0644	0 050268
0 03	60	0 8072	0.9993	0.0964	0 050268
0.03	60	0.8873	0.9995	0.0564	0.050268
0.025	0	0 5443	0.9996	0.2278	0 173900
0.025	0	0 4316	0.9982	0.2842*	0 173900
0 025	0	0 4262	0.9998	0 2869*	0 173900
0 025	0	0.413	0.9994	0 2935*	0.173900
0 025	20	0.737	0.999	0 1331	0.127546
0.025	20	0.7698	0 9993	0.1151	0.127546
0.025	20	0 8615	0.9997	0.0692*	0.127546
0.025	40	0 8323	0.9993	0.0839	0.081191
0 025	40	0.8321	0.9999	0.0840	0 081191
0.025	40	0.861	0.9997	0 0695	0.081191
0.025	60	0.8929	0.9997	0.0535	0.034837
0.025	60	0 9242	0.9997	0.0379	0.034837
0.025	60	1.0847	0.9997	−0.0423*	0.034837
0.02	0	0.655	0 9996	0.1725	0 158469
0.02	20	0 7591	0 9982	0.1204	0 112115
0 02	20	0 7532	0.9993	0 1234	0.112115
0 02	20	0 7534	0.9996	0.1233	0.112115
0 02	40	0 8568	0.9999	0 0716	0 065760
0 02	40	0 8415	0.9995	0 0793	0.065760
0 02	40	0.8467	0.9998	0 076	0.065760
0 02	40	0.9438	0.9999	0 0281	0.065760
0.02	50	0.874	0.9999	0.063	0.042583
0.02	60	0.931	0 9998	0.0345	0.019406
0.02	60	0.9314	0 9996	0.0343	0.019406
0 02	60	0.9074	0.9998	0 0463	0.019406
0 015	0	0.6574	0.9998	0.1713	0.143038
0.015	20	0 7954	0.9996	0.1022	0.096683
0.015	20	0.8911	0.9995	0.0544	0.096683
0.015	40	0 9138	0 9998	0.043	0 050329
0 015	40	0 9334	0.9995	0 0333	0.050329
0 015	40	1 0783	0.9996	−0.0391*	0.050329
0 015	60	1.1159	0.9985	−0 0579	0.003974
0.015	60	1.0263	0 9991	−0.0131	0 003974
0 015	60	0.9621	0.9991	0 0189	0.003974

* excluded data in regression analysis of Poisson's ratio

d : Density of geofoam (kg/m^3)

σ_3 : Confining pressure (kPa)

R^2 : Coefficient of determination

5. Conclusions

The use of geofoam for filling material to reduce earth pressure has been increased lately: however, the numerical model for geofoam behavior prediction has not studied properly. For example, long-term deformation behavior as a function of confining stress used as practical application criteria. Generally, short-term stress-strain behavior is predicted using linear elastic numerical model of initial tangent modulus at the initiative loading condition. However, the realistic stress-strain behavior is elasto-plastic typically. Proper numerical model for short-term behavior considering geofoam density and confining stress is essential to estimate long-term stability of various geofoam filling mass configurations. In this paper, non-linear elastic numerical model of geofoam through triaxial test is proposed and evaluated through experiments.

The conclusions of this study are as follows;

1) The geofoam shows an elasto-plastic behavior, and geofoam behavior has close relationship with density and confining stresses. Through a series of triaxial test of geofoam for various densities and confining stress, the axial stress and strain can be expressed as a function of geofoam density and confining stress.
2) In the proposed model, the parameters a and b have multi-linear relation, and parameter c has a nonlinear relation with geofoam density and confining stress.
3) The first derivative of proposed stress-strain relation, which represent the tangential modulus at that stress-strain level, can be expressed as a function of geofoam density and confining stress.
4) The volumetric strain and axial strain have a linear relation, and its slope is related with density and confining stress.
5) The Poisson's ratio has a multi-linear relation with geofoam density and confining stress, and its relation can be described as a certain function.

References

1. Bang, S. C., (1995), "Experimental and Analytical Study of Expanded Polystyrene Blocks in Highway Application", *Proceedings of*

International Seminar on the Application of EPS for Embankment Construction, Seoul, pp. 105-133.

2. BASF, (1995), "Code of Practice Using Expanded Polystyrene for the Construction of Road Embankments", *Technical Information from BASF*, pp. 7-9.
3. Cho, Y. K., (1992), "Behavior of Retaining Wall with EPS Blocks as Backfill", *Thesis of Master Course*, University of South Dakota, pp. 1-29
4. Chun, B. S., Jang, M. S., and Lim, H. S , (1996), "A Study on Engineering Characteristics of Load Reducing Material EPS", *Journal of the Korean Geotechnical Society*, Vol. 12, No. 2, pp 59-69.
5. Chun, B. S., Yoo, H.K., and Lim, H. S., (1996), "A Study on the Application of Numerical model to Predict Behavior of EPS", *Journal of the Korean Geotechnical Society*, Vol 12, No 6, pp. 185-195.
6. EPS Construction Methods Developing Organization, (1993), *EPS Construction Methods*, pp. 1-58.
7. Hamada, E. and Yamanouchi, T., (1989), "Mechanical Properties of Expanded Polystyrene as a Lightweight Fill Material", *Soils and Foundations*, Japan, pp. 13-18.
8 Horvath J. S. (1998), "Mathematical Modeling of the Stress-Strain-Time Behavior of Geosynthetics Using the Findley Equation", *General Theory and Application to EPS Block EPS*, Manhattan College Research Report No. CE/GE-98-3, U.S.A.
9. Kutara, K , Aoyama, N., Takeuchi, T., and Takechi, O, (1989), "Experiments on Application of Expanded Polystyrene to Light Fill Materials", *Soils and Foundations*, Japan, pp. 49-54.

(received on May., 4. 2000)